PHYSICAL REVIEW D **83,** 103528 (2011)

Role of shell crossing on the existence and stability of trapped matter shells in spherical inhomogeneous Λ-CDM models

Morgan Le Delliou*
Instituto de Física Teórica UAM/CSIC, Facultad de Ciencias, C-XI, Universidad Autónoma de Madrid, Cantoblanco, 28049 Madrid, Spain

Filipe C. Mena†
Centro de Matemática, Universidade do Minho, Campus de Gualtar, 4710-057 Braga, Portugal

José P. Mimoso‡
Departamento de Física, Faculdade de Ciências da Universidade de Lisboa, Centro de Astronomia e Astrofísica, Universidade de Lisboa, Campo Grande, Edifício C8 P-1749-016, Lisboa, Portugal
(Received 4 March 2011; published 27 May 2011)

We analyze the dynamics of trapped matter shells in spherically symmetric inhomogeneous Λ-CDM models. The investigation uses a generalized Lemaître-Tolman-Bondi description with initial conditions subject to the constraints of having spatially asymptotic cosmological expansion, initial Hubble-type flow, and a regular initial density distribution. We discuss the effects of shell crossing and use a qualitative description of the local trapped matter shells to explore global properties of the models. Once shell crossing occurs, we find a splitting of the global shells separating expansion from collapse into, at most, two global shells: an inner and an outer limit trapped matter shell. In the case of expanding models, the outer limit trapped matter shell necessarily exists. We also study the role of shear in this process, compare our analysis with the Newtonian framework, and give concrete examples using density profile models of structure formation in cosmology.

DOI: 10.1103/PhysRevD.83.103528 PACS numbers: 98.80.−k, 04.20.Jb, 95.30.Sf, 98.80.Jk

I. INTRODUCTION

Studies of nonlinear structure formation in cosmology, namely spherical top hat collapse models, often assume that there is no influence of the cosmological background on a finite domain which has disconnected from the background dynamics (see e.g. [1–4]).

We have looked at this problem in more detail in Ref. [5] and found local conditions under which such separation could be justified for inhomogeneous cosmological models. In particular, we have studied the possibility for perfect fluid solutions to exhibit locally defined separating shells between collapsing and the expanding (cosmological) regions.

The simplest examples given in [5] were set in an inhomogeneous universe of dust with a positive cosmological constant and the nature of the dust spherical shells allowed the system to be entirely determined from its initial conditions, at least, until the eventual occurrence of shell crossing.

However, shell crossings or caustics are expected to happen in these settings with more general initial conditions than in [5] and an interesting question is whether our previous results are robust with respect to the occurrence of shell crossing. This is the main concern in this paper, which can be regarded a natural follow-up of our previous work [5].

Shell crossing in spherical symmetry has already been studied in several past works, although in contexts different from the one of the present paper. For Lemaître-Tolman-Bondi (hereafter LTB) spacetimes, shell-crossing conditions were established by Hellaby and Lake [6] in terms of the metric data and more recently rewritten by Sussman in terms of quasilocal scalars [7,8]. Gonçalves [9], has shown that shell crossing exists for Λ-LTB spacetimes with charge. In [10], it has been shown that shell crossing occurs for a large class of initial conditions in models of formation of voids and some cases of fluids with pressure gradients.

There were also several works about the strength of shell-crossing singularities, with the general conclusion that it is a weak singularity in the sense of Tipler [11]. This then raised the question of the continuity of the metric across these singularities and, very interestingly, solutions of dynamical extension through shell-crossing singularities of LTB have been proved to exist, by Nolan [12], while the case including a cosmological constant and electric charges has been discussed by Gonçalves [9].

A complementary treatment was given by Nunez *et al.* [13] for metric extensions through shell crossing based on the interactions between shells, which translate in a conservation relation between mass and momenta, for

*Also at Centro de Física Teórica e Computacional, Universidade de Lisboa, Av. Gama Pinto 2, 1649-003 Lisboa, Portugal.
Morgan.LeDelliou@uam.es; delliou@cii.fc.ul.pt
†fmena@math.uminho.pt
‡jpmimoso@cii.fc.ul.pt

timelike massive shells. Physically, this conservation relation summarizes the microphysics of the fluid, however *for dust*, only purely gravitational interaction occurs between crossing shells; hence, *the rest mass of each shell is conserved* [14].

Here, we shall not deal with the problem of metric extensions after shell crossing and, motivated by the above results, we shall assume the validity of the field equations in between shell-crossing events and the continuity of the radial coordinates. Our main concern here will be to study the effects of shell crossing on the existence and stability of separating shells in spherical symmetry. In this paper, we shall also discuss the role of shear in the formation of shells which separate expanding from collapsing regions, we shall compare our results with Newtonian cases and give a concrete example of initial data which develops shell crossing and exhibits separating shells in a Λ-dust model.

The models considered in this paper obey the following properties: (a) spherically symmetric dust (the rest mass of infinitesimal pressureless shells is conserved under shell crossing) with a cosmological constant in the generalized LTB (GLTB) system; (b) Lagrangian treatment of the radial coordinates (assume there are metric extensions through shell crossings); (c) asymptotic spatial cosmological behavior (Friedmann-Lemaître-Robertson-Walker, hereafter FLRW, at spatial infinity); (d) initial Hubble-type flow (outgoing initial velocities); (e) regular initial density distribution (no finite mass for infinitely thin shell, and no singularity or zero density at the center).

The paper is organized as follows: in Sec. II we recall the conditions for the existence of matter trapped shells and study the role of shear on the existence of those shells in Λ-LTB models. Section III is devoted to the study of the effect of shell crossing in Λ-LTB models. In particular, we perform a dynamical analysis and separate this study into a local and global effects. We give concrete examples in Sec. IV before presenting the final conclusions.

II. TRAPPED MATTER SHELLS IN Λ-CDM

A. Conditions for the existence of trapped matter shells

In this section, we briefly recall some results of our previous paper [5] which did not consider shell crossings.

The GLTB system proposed in Refs. [5,15] has the following simple form for the case of a Λ-dust model where $P' = 0$ and $P = P_{\rm dust} = 0$ (here we set $G = 1 = c$, $\Lambda > 0$, α is the lapse function, $r(T, R)$ the areal radius, and E the energy[1] of spatial hypersurfaces)

$$ds^2 = -\alpha(t,R)^2 dt^2 + \frac{(\partial_R r)^2}{1+E(t,R)} dR^2 + r^2 d\Omega^2. \quad (1)$$

The Bianchi identities projected along and orthogonal to the timelike flow $n = \partial_t$ yield (P is the pressure, ρ the density, the prime $'$ denotes ∂_R, a dot $\dot{}$ stands for ∂_t, and Θ is the expansion along the flow)

$$\dot{\rho} = -(\rho + P)\Theta, \quad (2)$$

$$-\frac{P'}{\rho + P} = \frac{\alpha'}{\alpha} = 0 \Rightarrow \alpha dt = dt^* \Rightarrow \alpha = 1, \quad (3)$$

and the Einstein field equations (M is the Misner-Sharp mass [16], defined as $M = \int_0^R 4\pi\rho r^2 r' dR)^2$

$$\dot{E}r' = -2\dot{r}\frac{1+E}{\rho+P}P' = \mp 2\frac{1+E}{\rho+P}P'\alpha\sqrt{2\frac{M}{r} + \frac{1}{3}\Lambda r^2 + E} \quad (4)$$

$$\Rightarrow \dot{E} = 0, \quad E = E(R), \text{ unless there is shell crossing,} \quad (5)$$

$$\dot{M} = -\dot{r}4\pi P r^2 = \mp 4\pi P r^2 \alpha\sqrt{2\frac{M}{r} + \frac{1}{3}\Lambda r^2 + E} = 0 \quad (6)$$

$$\Rightarrow M = M(R), \text{ unless there is shell crossing,} \quad (7)$$

$$\dot{r}^2 = 2\frac{M}{r} + \frac{1}{3}\Lambda r^2 + E. \quad (8)$$

Time derivation of Eq. (8) gives a Raychaudhuri equation related to the generalized Tolman-Oppenheimer-Volkoff (gTOV) function of Ref. [5]:

$$\text{gTOV} = \frac{M}{r^2} - \frac{\Lambda}{3} r = -\ddot{r}. \quad (9)$$

The dynamical analysis detailed in Ref. [5] yields the motion of separated noncrossing shells in their respective effective potential,

$$E = V(r) \equiv -\frac{2M}{r} - \frac{\Lambda}{3} r^2, \quad (10)$$

where the unstable saddle point, for which gTOV $= 0$, gives a local separating shell (see [5], Figs. 1 and 2, and repeated in Fig. 1), in the case when the shell's energy reaches its critical value. This separating (or "cracking," by analogy with Herrera *et al.* [17]) shell is characterized by

$$r_{\rm lim} = \sqrt[3]{\frac{3M}{\Lambda}}, \quad (11)$$

$$E_{\rm lim} = -(3M)^{2/3}\Lambda^{1/3} = -\Lambda r_{\rm lim}^2, \quad (12)$$

while the energy follows

$$E = \dot{r}^2 + V(r). \quad (13)$$

Definition 1.—Local trapped matter shells in Λ-LTB are defined in GLTB coordinates as the locus $R_\star$ such that

[1] Actually, ${}^3R = -2\frac{(Er)'}{r^2}$ so E is related to the 3-curvature.

[2] In case of shell crossing, $\dot{E}$ can be nonzero as $r' = 0$ and M gets changed by the loss or gain of the mass from infinitesimal shell crossings, so $E = E(t, R)$ and $M = M(t, R)$, in that case.

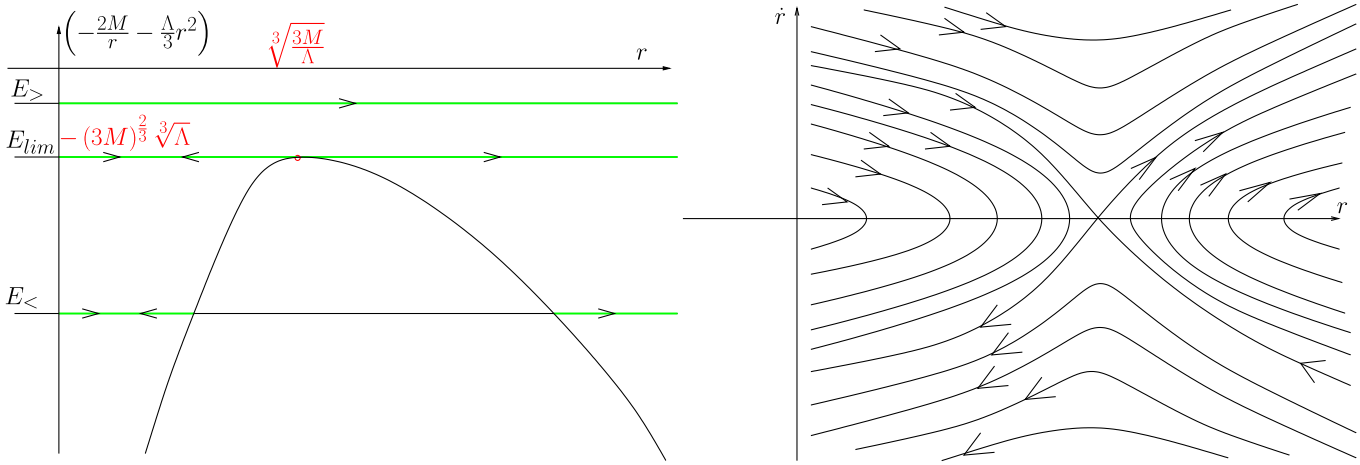

FIG. 1 (color online). Effective potential kinematic analysis (left) and phase space analysis (right) from [5]. The kinematic analysis for a given shell of constant M and E depict the fate of the shell, depending on E relative to $E_{\rm lim}$. It either remains bound ($E_< < E_{\rm lim}$) or escapes and cosmologically expands ($E_> > E_{\rm lim}$). There exists a critical behavior where the shell will forever expand, but within a finite, bound radius ($E = E_{\rm lim}$, $r \leq r_{\rm lim}$). The maximum occurs at $r_{\rm lim} = \sqrt[3]{3M/\Lambda}$. The corresponding phase space behavior follows, the scales are set by the value of $r_{\rm lim} = \sqrt[3]{3M/\Lambda}$ while the actual kinematic of the shell is given by E.

$$\frac{\Theta}{3}+a \equiv \frac{\dot{r}}{r}=0 \quad \text{and} \quad \mathcal{L}_n\left(\frac{\Theta}{3}+a\right) \equiv \left(\frac{\dot{r}}{r}\right)^{\cdot}=0. \tag{14}$$

□

This definition follows from Eqs. (3.11) and (3.16) of [5] applied to dust with Λ.

In Λ-LTB, conditions (14) are reached by shells at time infinity which are characterized by Eqs. (8) and (12) so that (see footnote 2) $E(t=\infty, R_\star) = E_{\rm lim}(t=\infty, R_\star)$ (defining $R_\star$) i.e.,[3]

$$\left(\frac{\Theta}{3}+a\right)^2 = 2\frac{M(R_\star)}{r^3(T,R_\star)}+\frac{1}{3}\Lambda-\frac{(3M(R_\star))^{2/3}\Lambda^{1/3}}{r^2(T,R_\star)}. \tag{15}$$

So, since here the Misner-Sharp mass M and energy E of each shell is conserved in time (without shell crossing), and E is thus set by initial $M(R)$ and $\dot{r}_i(R)$ profiles, one can characterize local trapped matter, or limit, shell by the intersections $E = E_{\rm lim}$ (see [5] for details). Global shells emerge from the neighborhood behavior around those intersections which local study we give in Secs. III A and III C.

Before studying the occurrence of shell crossing, we will now examine more carefully the role of shear in these settings.

B. The role of shear in the existence of trapped matter shells

In Ref. [5], we derived the relation between expansion and shear [see Eq. III.10] and found that, in the presently studied model, the shear could be put in the form

$$a = \mp\frac{1}{6\sqrt{E+2\frac{M}{r}+\frac{\Lambda}{3}r^2}}\times\left[\left(\frac{E'}{r'}-\frac{2E}{r}\right)+\frac{2}{r}\left(\frac{M'}{r'}-\frac{3M}{r}\right)\right]. \tag{16}$$

In the latter equation the terms within the brackets measure the departures from the profiles $E = \bar{E}(t)r^2$ and $M = \bar{M}(t)r^3$ that one would expect from a homogeneous, uniformly curved models. Indeed, in FLRW models $E = -kr^2$ and $M \propto \rho(t)r^3$. Moreover, we should stress that Eq. (16) yields the shear in terms of nonlocal (integral) quantities (E and M). We can now evaluate the expansion and shear at the limit shell defined by setting Eqs. (8) and (9) to zero at time infinity in Ref. [5], which, with the conservation of E and M, is simply defined by Eqs. (8) and (12). Combining those equations yields

$$E' = -\frac{2M'}{r_{\rm lim}}. \tag{17}$$

First on the limit shell we can write, setting $E = E_{\rm lim}$,

$$a = \mp\frac{\left\{2\frac{M'}{r'}\left(\frac{1}{r}-\frac{1}{r_{\rm lim}}\right)+2\Lambda\frac{r_{\rm lim}^2}{r}\left(1-\frac{r_{\rm lim}}{r}\right)\right\}}{6\sqrt{\frac{\Lambda}{3}\left(2\frac{r_{\rm lim}^3}{r}+r^2-3r_{\rm lim}^2\right)}}. \tag{18}$$

With the definition of mass issued from Eq. II.27 of Ref. [5] in GLTB coordinates so

$$M' = 4\pi\rho r^2 r', \tag{19}$$

we then express the shear of the limit shell as

$$a_{\rm lim} = \mp\sqrt{\frac{\Lambda}{3\left(\frac{r}{r_{\rm lim}}\right)^3}}\frac{1-\frac{4\pi\rho(r)}{\Lambda}\left(\frac{r}{r_{\rm lim}}\right)^3}{\sqrt{2+\frac{r}{r_{\rm lim}}}}, \tag{20}$$

[3]Erratum: Equation (3.14) of [5] has a sign typo. It should read

$$\text{gTOV} = -r\left[\mathcal{L}_n\left(\frac{\Theta}{3}+a\right)+\left(\frac{\Theta}{3}+a\right)^2\right].$$

which in the limit of time infinity simplifies into

$$a_{\lim\infty} = \mp\frac{\Lambda - 4\pi\rho(r_{\lim})}{3\sqrt{\Lambda}}. \tag{21}$$

This quantity does not vanish in general. Since at that locus we have $\Theta = 3(\frac{\dot{r}}{r} - a)$, the expansion then reads

$$\Theta_{\lim} = \pm\sqrt{\frac{3\Lambda}{\left(\frac{r}{r_{\lim}}\right)^3}}\left(\sqrt{2 - 3\frac{r}{r_{\lim}} + \left(\frac{r}{r_{\lim}}\right)^3} + \frac{1 - \frac{4\pi\rho(r)}{\Lambda}\left(\frac{r}{r_{\lim}}\right)^3}{\sqrt{2 + \frac{r}{r_{\lim}}}}\right), \tag{22}$$

which in the limit of time infinity simplifies into

$$\Theta_{\lim\infty} = \pm\frac{\Lambda - 4\pi\rho(r_{\lim})}{\sqrt{\Lambda}}. \tag{23}$$

We shall now use a particular form of initial data in order to study in more detail the role of shear in the appearance of the diving shell. In the examples below, we shall assume $M > 0$, $\rho > 0$, $\Lambda > 0$, and $E < 0$ around the origin.

So, consider analytic initial data for Λ-LTB as in [18,19]:[4]

$$\begin{aligned} M(R) &= R^3\sum_{i=0}^{\infty} m_i R^i, \qquad m_0 > 0 \\ E(R) &= R^2\sum_{i=0}^{\infty} E_i R^i, \qquad E_0 < 0 \end{aligned} \tag{24}$$

then, from the expressions above, we derive

$$\begin{aligned} a_{\lim}(R) &= \pm\Lambda^{1/2}\left(\frac{1}{3} - \frac{2}{3^{2/3}}\left(m_0^{1/3} + \frac{2m_1}{m_0^{2/3}}R + \left(\frac{3m_2}{m_0^{2/3}} - \frac{m_1^2}{m_0^{5/3}}\right)R^2 + O(R^3)\right)\right) \\ r_{\lim}(R) &= \left(\frac{3}{\Lambda}\right)^{1/3}\left(m_0^{1/3}R + \frac{m_1}{3m_0^{2/3}}R^2 + O(R^3)\right) \\ E_{\lim}(R) &= -3^{2/3}\Lambda^{1/3}\left(m_0^{2/3}R^2 + \frac{2m_1}{3m_0^{1/3}}R^3 + O(R^4)\right) \end{aligned} \tag{25}$$

also, for the rescaling $r(t_0, R) = R$, we get an expression for the initial shear distribution as (see also [20])

$$a(t_0, R) = \pm\frac{E_1 + 2m_1}{6A}R \pm \frac{1}{6}\left(\frac{2E_2 + 4m_2}{A} - \frac{(E_1 + 2m_1)^2}{2A^3}\right)R^2 + O(R^3)$$

with $A(R) = \sqrt{E_0 + \Lambda/3 + 2m_0}$.

It is interesting to see that for a fixed shell R near the center, bigger M (i.e. bigger m_3) means smaller initial shear but bigger $|E_{\lim}|$ and $r_{\lim}$ for that shell. On the other hand, since bigger initial shear implies smaller $|E_{\lim}|$ (i.e. smaller departures from $E_{\lim} = 0$) and smaller $r_{\lim}$, one can argue that, at least around the origin (and for the above initial data), shear contributes to the appearance of cracking limit shells. This is in agreement with the results of Herrera *et al.* [17]. We summarize this result as follows.

Result 1.—Consider a neighborhood U of the origin where the Λ-LTB initial data can be written as (24). Then, bigger values of the initial shear $|a(t_0, R)|$ in U, imply smaller $|E_{\lim}|$ and favor the occurrence of trapped matter shells in U. □

For data which is asymptotically Friedmann at infinity we take functions which, at infinity, can be expanded in the form:[5]

$$M(R) = \sum_{i=1}^{+\infty} m_i R^{3/i}, \qquad E(R) = \sum_{i=1}^{+\infty} E_i R^{2/i}$$

with $m_1 \neq 0$ and $E_1 \neq 0$. By taking asymptotic expansions we find

$$\begin{aligned} r_{\lim}(R) &= \left(\frac{3}{\Lambda}\right)^{1/3}\left(m_1^{1/3}R + \frac{m_2}{3m_1^{2/3}}\left(\frac{1}{R}\right)^{1/2} + O\left(\frac{1}{R}\right)\right) \\ E_{\lim}(R) &= -3^{2/3}\Lambda^{1/3}\left(m_1^{2/3}R^2 + \frac{2}{3}\frac{m_2}{m_1^{1/3}}R^{1/2} + \frac{2}{3}\frac{m_3}{m_1^{1/3}} + O\left(\frac{1}{R^{1/4}}\right)\right) \end{aligned} \tag{26}$$

while the initial shear is

$$a(t_0, R) = \mp\frac{E_2}{2\sqrt{3}\sqrt{3E_1 + \Lambda + 6m_1}}\frac{1}{R} + O\left(\frac{1}{R^{4/3}}\right).$$

So, again, bigger values of the initial shear $|a(t_0, R)|$ near infinity imply smaller $|E_{\lim}|$ and favor the occurrence of trapped matter shells.

We shall return to this issue in Sec. IV where we study other examples in more detail.

III. SHELL CROSSING AND TRAPPED MATTER SHELLS

A. Sufficient conditions for shell crossing

In terms of the comoving coordinates of metric (1), shell crossing is defined as a surface for which $\partial_R r = 0$ and the density diverges.[6] In geometrical terms, at shell crossing there is a discontinuity both in the extrinsic curvature K_{ij} and in the spacetime metric. For the spacetimes considered here, those discontinuities are finite and the magnitude of

[4]This data ensures that the solution approaches FLRW at the origin which is therefore regular.

[5]Note that we only assume this data form at infinity and not around the origin. Otherwise, we would have a nonregular origin.

[6]There can exist cases where $\partial_R r = 0$ and the density does not diverge. At those regular extrema, the extrinsic curvature is discontinuous while the metric is continuous and finite [6,21].

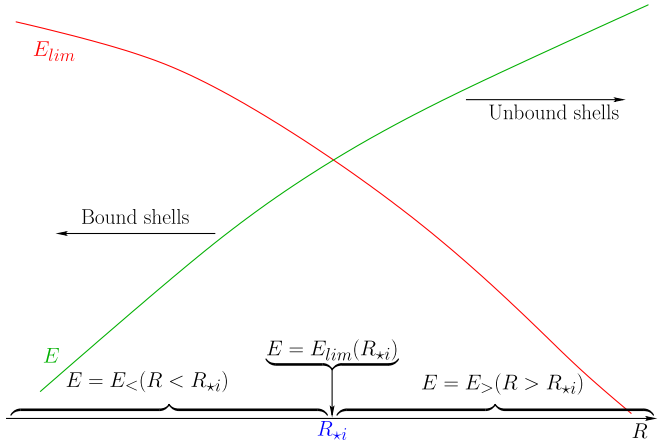

FIG. 2 (color online). Overcoming local configuration of E intersecting $E_{\rm lim}$. Phase space and effective potential trajectories from dynamical analysis of [5] give the local qualitative behavior, emphasized on the radial axis. Inner shells on bound trajectories and outer shells on unbound paths forecast no shell crossing locally. Considering $E_{\rm lim}$ as corresponding to the Newtonian zero radial velocity axis in [26,27], this configuration is analogous to, e.g., Fig. 1 of [31].

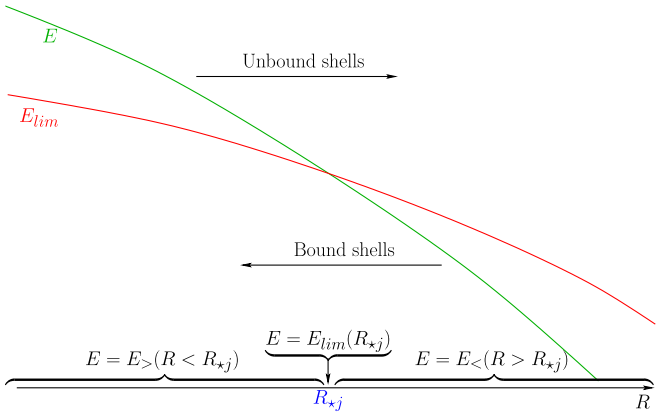

FIG. 3 (color online). Undercoming local configuration of E intersecting $E_{\rm lim}$. Phase space and effective potential trajectories from dynamical analysis of [5] give the local qualitative behavior, emphasized on the radial axis. Outer shells on bound trajectories and inner shells on unbound paths will lead to local shell crossing. Considering $E_{\rm lim}$ as corresponding to the Newtonian zero radial velocity axis in [26,27], this configuration is similar to, e.g., Fig. 2b of [26].

the jump in K_{ij} can be read from the expressions derived in [14,22].

Hellaby and Lake [6] (see also [23]) have derived necessary and sufficient conditions for the occurrence of shell crossing in LTB, in terms of the free initial data. Other works have used other types of conditions which are sufficient to avoid shell crossing[7] and therefore imply $\partial_R r \neq 0$. For example, in the case of LTB, Landau and Lifshitz [24] simply assume $\partial_R r > 0$ and, in [25], Hellaby and Lake impose the condition for a simultaneous big bang in their local analysis around the initial singularity.

Here, we shall take a different point of view and write sufficient conditions for the occurrence of shell crossing in terms of the local behavior of M and E in the neighborhood of some intersection, when it exists, of the energy E with the critical energy $E_{\rm lim}$. In order to do that we first observe that two local configurations are possible in the neighborhood of the intersection: either $E' > E'_{\rm lim}$ or $E' < E'_{\rm lim}$.

In the case $E' > E'_{\rm lim}$, shells just inside the intersection radius will have a lower E than their respective $E_{\rm lim}$ and will therefore be trapped in closed trajectories, following the dynamical analysis presented in Fig. 1. In that case, shells just outside the intersection will display higher E than their respective $E_{\rm lim}$ and will accordingly be free to escape to infinity on unbound trajectories. That shell distribution will lead to the separation of neighboring shells, those inside the intersection being bound to a finite region while those outside will escape to infinity. This case does not entail neighboring shell crossings and is presented on Fig. 2.

On the contrary, in the case $E' < E'_{\rm lim}$, shells just inside the intersection will have a higher E than their respective $E_{\rm lim}$ and will accordingly be free to escape to infinity on unbound trajectories, whereas shells just outside the intersection will display a lower E than their respective $E_{\rm lim}$ and will therefore be trapped in closed trajectories. Because of the configuration of that shell distribution, shell crossings of neighboring shells occur: those inside the intersection escaping to infinity will have to cross those outside which are bound to a finite region. This case is presented on Fig. 3. We summarize this result as follows

Result 2.—Let $\Delta = E - E_{\rm lim}$ and consider a Λ-LTB spacetime where there is $R_\star$ such that $\Delta|_{R_\star} = 0$. Then, a sufficient condition for the existence of shell crossing is $\Delta'|_{R_\star} < 0$. □

We point out that, for $\Lambda = 0$, our condition leads to $E' < 0$, which is the condition implicitly considered in [6,23].[8] In that case, we simply obtain $E'_{\rm lim} = -8\pi\rho r^2 r'(\frac{\Lambda}{3M})^{1/3} = 0$. In this sense, our sufficient

[7]A comment on the occurrence of caustics when using a synchronous reference frame can be found in Ref. [24] (Sec. 97). We must notice though that the latter assumes that the strong energy condition holds, whereas in our present case the cosmological constant evades that assumption.

[8]For LTB with $\Lambda = 0$, we recall that the necessary and sufficient conditions for no-shell crossing in [6] are

$$T'_B \leq 0, \qquad E' \geq 0, \qquad M' \geq 0,$$

where T_B is the bang time, while the necessary and sufficient conditions for no-shell crossing in [23] are

$$T'_B \leq 0, \qquad E' > 0, \qquad M' \geq 0.$$

Therefore, if one of these conditions fails then there will be shell crossing.

condition generalizes, for $\Lambda \neq 0$, the result of Ref. [6,23].[9] We also note that their condition on bang times $t_b(R)$ is $t_b'(R) \leq 0$, while we can also allow for $t_b'(R) > 0$ as long as $t_b(R)$ is less than the initial time t_0 considered here.

There is an interesting analogy between our shell-crossing condition and a similar condition in Newtonian theory. In fact, the Newtonian approach used in [26,27] considers kinematic configurations in velocity-radius two-dimensional phase space which lead to one-(and three-) dimensional Zel'Dovich pancakes (see Refs. [27–29] for the classical cosmological spherical context). Their behavior is similar to the local evolutions of the dynamical configurations in Figs. 2 and 3. While in [26,27] the authors take the radial axis to separate collapsing and expanding kinematics, here we take $E_{\rm lim}$ locally as a deformed radial axis.

B. Hypotheses and dynamical analysis

Since part of our analysis is based on the $E - E_{\rm lim}$ diagram, it is useful to clarify the constraints introduced by the set of hypotheses we propose.

1. Regular density distribution

A regular density distribution is motivated by standard cosmological models ([10,28], for example). In the weak energy condition, the density remains positive so the mass profile is initially always monotonously increasing, thus $E_{\rm lim}$, from Eq. (12), is initially always monotonously decreasing,

$$\frac{\partial M}{\partial R} \geq 0 \Rightarrow \frac{\partial E_{\rm lim}}{\partial R} \leq 0. \tag{27}$$

The regularity implies finiteness of the mass and nonzero values for the density at the center. This constrains their logarithmic slope in the following manner: suppose a value $-\epsilon$ for the slope of the density in the center ($\rho \propto r^{-\epsilon}$), then the mass shall behave accordingly as $r^{3-\epsilon}$. Finiteness of the mass implies then $\epsilon \leq 3$ and no vacuum in the center implies $\epsilon \geq 0$, from the density.

2. Initial Hubble-type flow

This simplifies the initial velocity profile into one that only admits outgoing radial velocities (positive $\dot{r}$), in the fashion of expanding initial conditions in a Hubble flow, although less restrictive. As a consequence of this and the previous condition, the profiles in the center always respect, in initial conditions, the hierarchy $E < E_{\rm lim}$, which is crucial for the emergence of a bound core. In this case

$$E_{\rm lim} = -(3M)^{2/3}\Lambda^{1/3} \underset{R\to 0}{\sim} R^{2-(2/3)\epsilon} \to 0 \quad \text{as } \epsilon \leq 3,$$

$$E = \dot{r}^2 - \frac{2M}{R} - \frac{\Lambda}{3}R^2 \underset{R\to 0}{\sim} -R^{2-\epsilon} \to 0,$$

since $\dot{r} \underset{R\to 0}{\sim} R \to 0$ so the $\dot{r}^2$ and $\frac{\Lambda}{3}R^2$ both tend to zero as R^2 and are thus dominated by the $-\frac{2M}{R}$ term for $\epsilon > 0$. Thus around the center,

$$\frac{E}{E_{\rm lim}} \underset{R\to 0}{\simeq} \frac{2}{3^{2/3}R}\left(\frac{M}{\Lambda}\right)^{1/3} \underset{R\to 0}{\sim} \frac{2}{3^{2/3}\Lambda^{1/3}}R^{-(\epsilon/3)} > 1$$

$$\Rightarrow E < E_{\rm lim}, \quad \text{for } \epsilon > 0, \quad E_{\rm lim} < 0.$$

In the peculiar case of a constant central density ($\epsilon = 0$), we have $M \underset{R\to 0}{\sim} \frac{4\pi}{3}\rho_0 R^3$, $\dot{r} \underset{R\to 0}{\sim} \partial_R \dot{r}_0 R = H_c R$, so $E = (H_c^2 - \frac{8\pi}{3}\rho_0 - \frac{\Lambda}{3})R^2 = (H_c^2 - \frac{8\pi}{3}(\rho_0 + \rho_\Lambda))R^2$. In that case, the Hubble-type flow needs to remain moderate in the center to respect the constraint

$$\partial_R \dot{r}_0 < 4\pi(\rho_0^{2/3}(2\rho_\Lambda)^{1/3} + \tfrac{2}{3}(\rho_0 + \rho_\Lambda)).$$

In the rest of the paper, we assume the conditions for $E < E_{\rm lim}$ in the center are met.

3. Asymptotic spatial cosmological behavior

If we restrict our explorations to *asymptotically cosmological* (FLRW) solutions, this implies that at radial infinity the mass and velocity initial profiles, constraining the energy and $E_{\rm lim}$ profiles for all time, shall obey

$$M \underset{R\to\infty}{\to} \frac{4\pi}{3}\rho_b R^3 \ \text{ with } \frac{3M}{4\pi R^3} \underset{R\to\infty}{\to} \rho_b = \rho_b(t)$$

$$\Rightarrow E_{\rm lim} \underset{R\to\infty}{\to} -(4\pi\rho_b)^{2/3}\Lambda^{1/3}R^2,$$

$$\dot{r}_i(R) \underset{R\to\infty}{\to} H_i R \Rightarrow E \underset{R\to\infty}{\to} -KR^2. \tag{28}$$

We note that the value of the curvature K of the asymptotic FLRW solution compared with the equivalent $(4\pi\rho_b)^{2/3}\Lambda^{1/3}$ FLRW critical curvature will determine, together with the central constraint $E < E_{\rm lim}$, the occurrence of, at least, one intersection of E and $E_{\rm lim}$ of the $E' > E'_{\rm lim}$ kind, not inducive of shell crossing (see Sec. III A).

Definition 2.—Supposing there exists $n \in \mathbb{N}$ shells verifying Eq. (15), we order them by initial radius and denote them $R_{\star i}$, $i \in [1, n]$,

(i) $R_{\star \rm out} \equiv R_{\star n}$ the outermost intersections $E = E_{\rm lim}$ of the initial profiles

(ii) $R_{\star \rm in} \equiv R_{\star 1}$ the innermost initial intersections $E = E_{\rm lim}$ of the initial profiles. □

4. Local mass conservation and Lagrangian frame

Since in our system the cosmological constant is inert by definition and dust purely interacts gravitationally, we assume, as in [14], that *the rest mass of each crossing infinitesimal shell is conserved*. The shell-crossing event can thus be viewed as an infinitesimal exchange of the relative positions and integrated masses while each shell conserves its own velocity.

As shell masses M and energies E are conserved between shell-crossing events, Eq. (8) will govern the motion

[9] Although our interest is in the neighborhood of radius where $\Delta = 0$, our analysis can be extended to other locations.

of individual shells. Keeping initial $R = r(0, R)$ as Lagrangian labels, we can follow the dynamics of the shells using the simple prescription obtained above without the need to reorder the radial labels as would require a metric extension. Instead, we keep the initial labels all throughout and follow each shell's evolution using Eq. (8) and the shell-crossing prescription of Sec. III B 4, as e.g. in Refs. [26,28].

C. Local effects of shell crossing on trapped matter shells

In this section, we will detail how a test crossing shell affects locally the values of E and $E_{\rm lim}$ around trapped matter shells.

Since each shell conserves its infinitesimal mass, the local effect of an elementary crossing of a system's shell by a test, neighboring, shell will just exchange their nonlocal mass in the exchange of their positions.[10] As a consequence, their values of E and $E_{\rm lim}$ will also change. The change of E, in Eq. (4), is allowed by the shell-crossing event.

A shell crossed at some $r_\times$ by an infinitesimal mass δM ($\delta M > 0$ for inward crossing, <0 for outward crossing) will see its values shifted as follows (the reciprocal is true for the crossing shell with $-\delta M$):

$$E_{+\delta} = E - \frac{2\delta M}{r_\times}, \tag{29}$$

$$E_{\rm lim+\delta} \simeq E_{\rm lim} + \frac{2}{3}\frac{\delta M}{M} E_{\rm lim}. \tag{30}$$

Thus, for an inward (respectively outward) crossing, both E and $E_{\rm lim}$ will decrease (respectively increase). Their relative separation, crucial around intersections, will follow

$$\delta\Delta \simeq 2\delta M\left(\frac{1}{r_{\rm lim}} - \frac{1}{r_\times}\right), \tag{31}$$

which generalizes the conditions from [6,23] (see Result 2). The sign of this shift is determined by the initial position $r(t_0, R) = R = r_i$ of shells with respect to their $r_{\rm lim}$.

Bound shells can never cross their respective $r_{\rm lim}$ and shells with $E = E_{\rm lim}$ reach their $r_{\rm lim}$ at infinity in time. Thus, crossing events involving one bound shell satisfy $\left(\frac{1}{r_{\rm lim}} - \frac{1}{r_\times}\right) < 0$. However, once escaping shells go beyond their respective $r_{\rm lim}$, they experience the opposite relative effect on their $\delta\Delta$. Thus, it is possible to have a crossing of two escaping shells beyond their respective $r_{\rm lim}$ that produce shifts in the opposite direction. However, once beyond their $r_{\rm lim}$, even drastic changes cannot put shells on closed orbits linked with the center as they would correspond to points on the outer side of the effective potential [Fig. 1(a)]. Since intersections $E = E_{\rm lim}$ take place in the neighborhood of bound shells (those with E under their $E_{\rm lim}$), we can restrict ourselves to consider local shell crossing in $r_\times < r_{\rm lim}$.

[10] In this process the other shells of the system, not involved, will remain unaffected and conserve their masses.

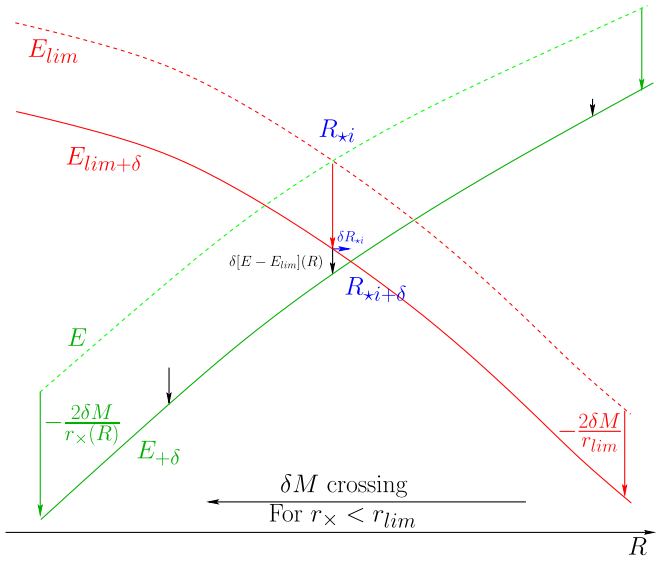

FIG. 4 (color online). Effect of an ingoing, infinitesimal test shell crossing on the energy and critical energy profiles, around the *local* initial configuration for the overcoming of $E_{\rm lim}$ by E. The initial intersection shell becomes bound on such perturbations and the local intersection shell shifts outwards in radius.

To first order, for inward-going crossing shells, we have $\delta\Delta < 0$, as illustrated on Figs. 4 and 7, while outward-going shells have $\delta\Delta > 0$, see Figs. 5 and 6. As a consequence, the limit shell defined by the intersection shifts forward (respectively backward) for the two cases of local configurations. The resulting cases are overcoming inward

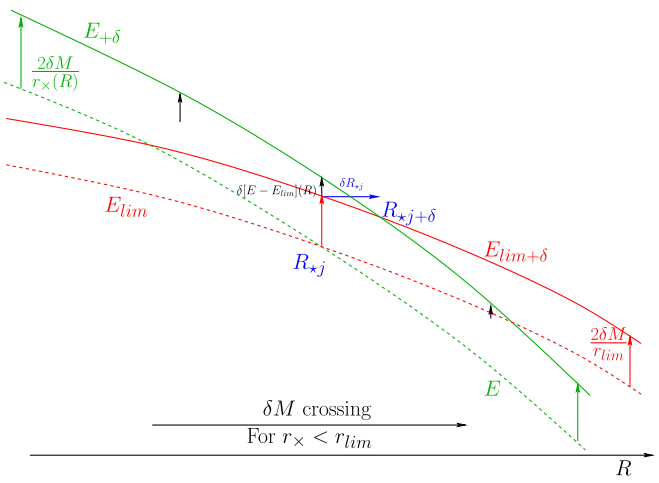

FIG. 5 (color online). Effect of an outgoing, infinitesimal shell crossing on the energy and critical energy profiles, around the *local* initial configuration for the undercoming of $E_{\rm lim}$ by E. The initial intersection shell becomes unbound on such perturbations and the local intersection shell shifts outwards in radius.

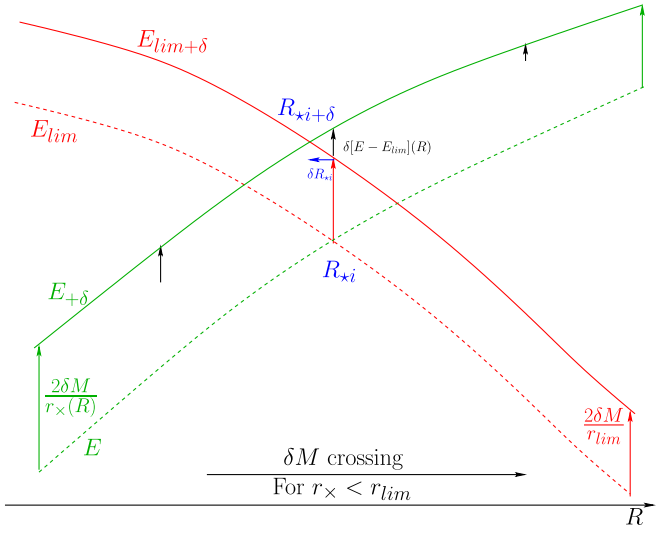

FIG. 6 (color online). Effect of an outgoing, infinitesimal shell crossing on the energy and critical energy profiles, around the *local* initial configuration for the overcoming of $E_{\rm lim}$ by E. The initial intersection shell becomes unbound on such perturbations and the local intersection shell shifts inwards in radius.

crossings and undercoming outward crossings (respectively overcoming outward crossings and undercoming inward crossings) and are illustrated on Figs. 4 and 5 (respectively 6 and 7).

To simplify the qualitative study of the system, we will first consider a prescription where both M and E are conserved, in Secs. III D 1 and III D 2. We will then drop this assumption and include the evolution of trapped matter shells' neighborhoods, building from infinitesimal shell crossing as described below in Sec. III D 3 to ascertain the qualitative evolution of the system, in Sec. III D 4.

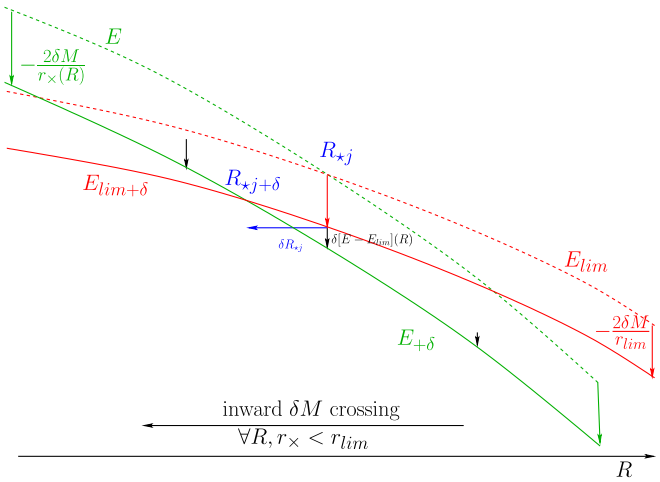

FIG. 7 (color online). Effect of an ingoing, infinitesimal test shell crossing on the energy and critical energy profiles, around the *local* initial configuration for the undercoming of $E_{\rm lim}$ by E. The initial intersection shell becomes bound on such perturbations and the intersection shell shifts inwards in radius.

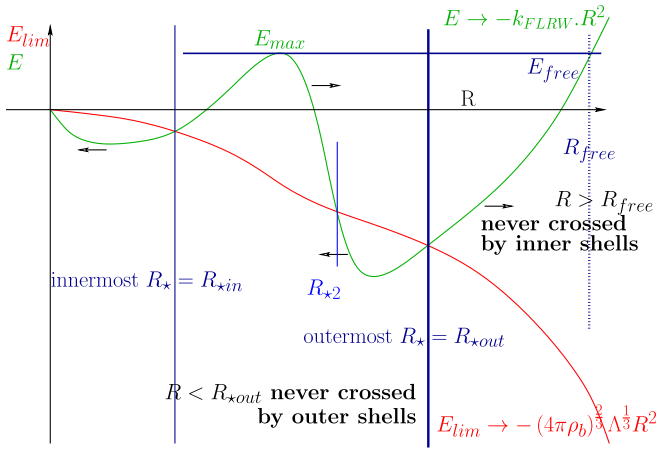

FIG. 8 (color online). Open background with arbitrary central mass distribution and a single local undercoming intersection. It always gives protected inner shells as well as unmodified cosmological expansion, when keeping integrability despite shell crossing. Shell crossing entails no fundamental modification.

D. Global effect of shell crossing on limit trapped matter shells

1. Simplest model with shell crossing

In order to study the simplest set of initial conditions where shell crossing occurs, given the constraints of Sec. III B from Result 2, we shall consider a model with a single undercoming configuration. The topological constraints coming from the two-dimensional E vs R diagrams,[11] together with the choice of an open background at infinity[12] leads to initial conditions for E and $E_{\rm lim}$ with three intersections (see Fig. 8), the middle one verifying Result 2. We thus have a model with $R_{\star 1} = R_{\star \rm in}$, $R_{\star 2}$ and $R_{\star 3} = R_{\star \rm out}$ defined in its initial conditions. We can now consider the *inner system*, also called *the system*, to be circumscribed by $R_{\star \rm out}$. Unbound shells inside this system are in position to escape it and, hence, define a remarkable shell outside the system:

Remark 1.—The inner or nonbound shells of initial conditions in E and $E_{\rm lim}$ induce a few remarkable features defined as follows:

(i) We will consider all shells inside $R_{\star \rm out}$ as the initial inner system.

(ii) We will denote by $E_{\rm max}$ the maximum value of nonbound E in the set of shells inside $R_{\star \rm out}$ or outside of it but with horizontal tangent, i.e. $E_{\rm max} = \max\{E: ((E' = 0) \vee (0 < R \leq R_{\star \rm out})) \wedge (E \geq E_{\rm lim})\}$.

(iii) $R_{\rm max}$ is the largest value for which $E = E_{\rm max}$, i.e. $R_{\rm max} = \max\{R: E(R) = E_{\rm max}\}$.

[11] For example, in the center, we have $(E < E_{\rm lim})$. See Fig. 8.

[12] This means $E \underset{R\to\infty}{\longrightarrow} -k_{\rm FLRW}R^2$ with $k_{\rm FLRW} < 0$ and $E_{\rm lim} \underset{R\to\infty}{\longrightarrow} -(4\pi\rho_b)^{2/3}\Lambda^{1/3}R^2$.

(iv) R_{free} is the furthest shell outside $R_{\star\text{out}}$ with increasing $E = E_{\max}$, when it exists, i.e. $R_{\text{free}} = \max\{R\colon (R \geq R_{\star\text{out}}) \wedge (E = E_{\max}) \wedge (E'(R) > 0)\}$.
(v) We will note E_{free} the value of E, when it exists, as $E_{\text{free}} = E(t = t_0, R_{\text{free}})$. □

With the above definitions, we will now examine the effects of shell crossing on trapped matter shells.

2. Limit trapped matter shells in the integrable dynamical system

In a model where both M and E are conserved through shell crossings, we can extend the analysis of [5], as each shell's dynamics remains integrable and is governed by the Lagrangian Eq. (8).[13] In this case, the qualitative dynamical behavior of the system is entirely determined from the shape of its initial conditions in a E and $E_{\lim}$ vs R diagram.

As we will see in Sec. III D 4, when including the full effects of shell crossing on E and $E_{\lim}$, the key properties of trapped matter shells will be obtained in the limit $t \to \infty$. Since in this section, M and E are assumed to be conserved with time, all the properties deduced here will remain unchanged in that limit. We will therefore express our results in the limit $t \to \infty$, using definitions which evolve from Remark 1 and are detailed in Appendix A.

From Fig. 8, we can see that all the bound shells will remain under $r_{\lim\star\text{out}} = r_{\lim}(R_{\star\text{out}})$, while all unbound shells of the inner system will escape it.[14] Thus, considering that bound shells will eventually turn around and orbit back and forth between the center and their turnaround radius, we find that all shells inside $r(t, R) = r_{\lim\star\text{out}}$ will be crossed from both sides (interior and exterior).[15] Only the shell $R_{\star\text{out}}$ will remain uncrossed from outside shells. This leads to the following definition.

Definition 3.—The outer limit trapped matter shell $R_{t\star\text{out}\infty}$ verifies Definition 1 in the limit $t \to \infty$, in addition to being the outermost such shell which locally is not shell-crossing inducive,[16] i.e.,

$$R_{t\star\text{out}\infty} = \{R\colon \max\{R_{\star\infty}\} \wedge (E'(t \to \infty) > E'_{\lim}(t \to \infty))\}.$$

□

Note, from Definition 2, that $R_{\star\text{out}}$ verifies Definition 3, defines $R_{t\star\text{out}}$, if $E' > E'_{\lim}$, and verifies $R_{t\star\text{out}} = R_{t\star\text{out}\infty}$ in the limit $t \to \infty$.

Remark 2.—In Λ-LTB with asymptotic cosmological evolution (FLRW at radial infinity) and initial Hubble-like flow (outwards going) for which shell crossing occurs, the outer limit trapped matter shell is a surface S with the following properties:

(i) The matter exterior to S follows trapped geodesics, remaining in that exterior.
(ii) The matter inside S can expand and collapse protected from the crossing of outside shells.
(iii) S is the shell with largest R for which the energy E intersects the critical energy $E_{\lim}$, from bound to unbound shells. □

The condition for existence of $R_{t\star\text{out}\infty}$ follows from the properties of $R_{t\star\text{out}}$, so we obtain the following result.

Result 3.—Sufficient conditions for the existence of an outer limit trapped matter shell are:

(i) The FLRW curvature of the background $k_{\text{FLRW}} < (4\pi\rho_b)^{2/3}\Lambda^{1/3}$, or
(ii) $R_{t\star\text{out}}$ exists, or
(iii) the local configuration around $R_{\star\text{out}}$ is such that $E'_{\star\text{out}} > E'_{\lim\star\text{out}}$.

Proof.—$k_{\text{FLRW}} < (4\pi\rho_b)^{2/3}\Lambda^{1/3} \Rightarrow E(R \to \infty) > E_{\lim}(R \to \infty)$ so the last intersection $E(R) = E_{\lim}(R)$ is such that $E' > E'_{\lim}$ from a corollary to Bolzano-Weierstrass theorem and Definition 3 is verified. □

We show, in Fig. 8, a diagram with data such that the inner limit trapped matter shell $R_{t\star\text{out}}$ is at $R_{\star\text{out}}$. The exterior of the system will include all the unbound shells escaping to infinity. However, the dynamics from Eq. (8) allows us to study under what conditions the unbound system's shells will never cross shells located in the exterior of the system.[17] Take two different shells $R_1 < R_2$, eventually crossing each other at a given radius[18] $r_\times$, and with the outer shell more open than the inner shell (i.e. $E_1 < E_2$ for $M_1 < M_2$):

$$E_1 = v_1^2 - \frac{\Lambda}{3}r_\times^2 - \frac{2M_1}{r_\times}, \quad \text{with } E_1 < E_2, \tag{32}$$

$$E_2 = v_2^2 - \frac{\Lambda}{3}r_\times^2 - \frac{2M_2}{r_\times} \quad \text{and} \quad M_1 < M_2, \tag{33}$$

$$\Rightarrow \Delta v^2 = \Delta E + \frac{2\Delta M}{r_\times} > 0 \quad \text{and} \tag{34}$$

$$\Delta v^2 \underset{r_\times \to \infty}{\sim} \Delta E > 0 \qquad \Rightarrow \forall t,\ v_2^2 > v_1^2. \tag{35}$$

Then shells with $E_1 < E_2$ and $M_1 < M_2$ will always remain in the same radial order and the shell with $E = E_{\max}$ will then escape all other system's shells. It then appears that, when R_{free} exists, all shells with $E > E_{\text{free}}$ will never be crossed by any shell inside R_{free}. The counterpart to Definition 3 can thus be formulated by defining first $E_{\max}$. In turn, the condition for the existence of $E_{\max}$ is that

[13]The final fate of each shell will always remain on horizontal lines and their gravitational nature, whether bound or unbound will also remain the same throughout their history.
[14]This is indicated on Fig. 8 by horizontal arrows.
[15]This includes the $R_{\star\text{in}}$ and $R_{\star 2}$ shells, locally considered trapped matter shells.
[16]Recall that $R_{\star\infty}$ is defined by solutions in initial R of Eq. (15) taken at $t \to \infty$.
[17]Their escape velocity at infinity should never exceed that of exterior shells.
[18]This radius is allowed to tend to radial infinity.

$E \geq E_{\rm lim}$, in the limit $t \to \infty$. Thus, Remark 1 can be adapted here as follows.[19]

Definition 4.—Suppose $E_{\max\infty}$ exists and is defined, in the initial conditions, as

$$E_{\max\infty} = \max\{E|_{(t\to\infty)}: ((E'=0)\vee(0<R\leq R_{\star{\rm out}\infty})) \wedge (E\geq E_{\rm lim})_{(t\to\infty)}\}. \quad (36)$$

Then, inner limit trapped matter shells are defined as the locus $R_{{\rm free}\infty}$ such that

$$R_{{\rm free}\infty} = \max\{R: (R\geq R_{\star{\rm out}\infty}) \wedge (E=E_{\max\infty})_{t\to\infty} \wedge (E'(t\to\infty, R)>0)\}. \quad (37)$$

□

Remark 3.—In Λ-LTB with asymptotic cosmological evolution (FLRW at radial infinity) and initial Hubble-like flow (outwards going) for which shell crossing occurs (and $E_{\max\infty}$ is defined), the inner limit trapped matter shell is a surface S with the following properties:

(i) The matter interior to S follows trapped geodesics which remain in that interior.
(ii) The matter exterior to S expands, protected from the crossing of inside shells.
(iii) S is the shell outside the system (defined with $R_{\star{\rm out}\infty}$) with energy equal to that of the highest E of nonbound shells, and starting inside of the system, or outside of it but with horizontal tangent. □

The conditions for existence of $R_{{\rm free}\infty}$ combine the existence of $E_{\max\infty}$ with constraints on the background:

Result 4.—Sufficient conditions for the existence of an inner limit trapped matter shell are (a) the existence of $E_{\max\infty}$ and (b) the existence of $E_{{\rm free}\infty}$:

(a)
(i) There exists initially a nonbound, system shell, or a nonbound shell with horizontal tangent: $\exists R$: $(0<R\leq R_{\star{\rm out}}\vee E'=0)\wedge E(R)\geq E_{\rm lim}(R)$, or
(ii) $R_{\star{\rm out}\infty}$ exists, or
(iii) There exist at least one $R_{\star i}$
(b)
(i) $E_{\max\infty} < E(R\to\infty)$, or
(ii) $\exists R$: $R\geq R_{\star{\rm out}\infty}\wedge E(t\to\infty, R)=E_{\max\infty}\wedge E'(R)>0$

Proof.—(a)
(i) If we have R such that $(0<R\leq R_{\star{\rm out}}\vee E'=0)\wedge E(R)>E_{\rm lim}(R)$, then, either it is a maximum so $E_{\max}$ exists and, by time evolution of its neighborhood, $E_{\max\infty}$ exists, or, by continuity, in the case when it is not a shell with $E'=0$ (local maximum), there is a shell with larger E which satisfies Remark 1 for $E_{\max}$ and thus one in its neighborhood satisfying Definition 5 for $E_{\max\infty}$.
(ii) If $R_{\star{\rm out}\infty}$ exists, it is not bound at time infinity and is inside the system; therefore, even if it is the only unbound system shell, it can at least define $E_{\max\infty}$.
(iii) If there is only one $R_\star$, then it is $R_{\star{\rm out}}$ by Definition 2. We are then in the case (ii) above as this guarantees the existence of $R_{\star{\rm out}\infty}$.

(b) Since:
(1) $E_{\max\infty}$ is, by definition, the largest value of E reached at time infinity by inner or outer local maxima shells,
(2) uncrossed outer shells have their E conserved,
(3) asymptotic cosmological conditions render E monotonous near infinity,
(4) evolution of the inner shell $R_{\max\infty}$ follows Eq. (35),
(5) the energy profile is continuous,

therefore, $E_{\star{\rm out}\infty}\leq E_{\max\infty}$ and by continuity, since $E_{\max\infty}<E(R\to\infty)$, exterior shells will obey $E\in[E_{\star{\rm out}\infty}, E(t\to\infty, R\to\infty)[\supseteq[E_{\max\infty}, E(t\to\infty, R\to\infty)[$, thus there exists at least one shell at time infinity with $E=E_{\max\infty}$.

Moreover, for the outermost exterior shell $R_{x\max\infty} = \max\{R: R\geq R_{\star{\rm out}\infty}, E(R)=E_{\max\infty}\}$ with $E=E_{\max\infty}$, since $E_{\max\infty}<E(R\to\infty)$, by continuity, all shells outside of it will verify $E>E_{\max\infty}$. Therefore $E'(R_{x\max\infty})>0$ and $R_{x\max\infty}=R_{{\rm free}\infty}$ is fulfilling Definition 4. □

We show a diagram in Fig. 8 where we indicate the outer limit trapped matter shell for which $R_{\rm free}=R_{{\rm free}\infty}$, in the model where both E and M are conserved between shell crossings. We thus have found, for that model, that extending the analysis of [5] in the context of shell crossing leads to the emergence of two remarkable shells: an inner limit trapped matter shell and an outer limit trapped matter shell. From their definitions 3 and 4, we can deduce other properties depending on the background cosmological model, namely:

From Result 3, any background with $E>E_{\rm lim}$ will admit an outer limit trapped matter shell. This includes some closed models and all flat and open models.

From Result 4, and under the assumptions of this section, any closed background in our models cannot foster an inner limit trapped matter shell as the finite value of $E_{\max\infty}$ is always larger than its energy at radial infinity. Conversely, open models always have an inner limit trapped matter shell (see the example of Sec. IV) and only flat models with moderate enough energy fluctuations [i.e. for which $E_{\max}<0=E(R\to\infty)$] can allow the existence of an inner limit trapped matter shell. In summary:

Summary 1.—Consider a Λ-LTB spacetime with asymptotic cosmological evolution (FLRW at radial infinity) and initial Hubble-like flow (outwards going) for which shell crossing occurs. Then:

(i) The global limit trapped matter shell found in the no-shell crossing Λ-LTB examples of [5] is split, if shell crossing occurs, into at most, two global shells, namely an inner limit trapped matter shell and an outer limit trapped matter shell.

[19]The following can be formulated also in terms of gauge invariant Lie derivatives, expansion and shear, as seen in Appendix B.

(ii) For open or flat expanding spacetimes,
  (a) there exists always an outer limit trapped matter shell at $R_{t\star\text{out}\infty}$.
  (b) The inner limit trapped matter shell exists in flat backgrounds for sufficiently small initial velocities inside the system limited by $R_{\star\text{out}\infty}$.

(iii) For closed spacetimes, outer limit trapped matter shells are present if $k_{\text{FLRW}} < (4\pi\rho_b)^{2/3}\Lambda^{1/3}$ and inner limit trapped matter shells cannot be defined if shell crossing occurs, with our definitions.

(iv) In the Λ-CDM examples of global limit trapped matter shells found in [5], inner and outer limit trapped matter shells reduce to one single surface.

Proof.—

(i) Direct from Definitions 3 and 4 and Result 2 which leads to shell crossings at some $R_\star$.

(ii)
  (a) From Result 3.
  (b) Direct from Result 4, as open and flat expanding spacetimes admit $E(R \to \infty) \geq 0$. Some flat spacetimes can exhibit $E_{\text{free}\infty} > 0$ while their $E \underset{R\to\infty}{\longrightarrow} 0$. For those cases, Definition 4 is never verified.

(iii) Using Result 3, for closed spacetimes, $E \underset{R\to\infty}{\longrightarrow} -\infty \ll E_{\text{free}\infty}$, so from Result 4, Definition 4 is never verified.

(iv) Applying Definitions 3 and 4 to configurations where there is only one intersection $R_\star = R_{\star 1} = R_{\star\text{out}}$ verifying $E' > E'_{\text{lim}}$, no shell crossing occurs. Thus, all E values are constant over time so $R_{\star\text{out}} = R_{t\star\text{out}\infty}$, and given the open background, $E_{\text{free}} = E_{\star\text{out}}$, so $R_{\text{free}\infty} = R_{\star\text{out}} = R_{t\star\text{out}\infty}$. □

In this section, we have assumed that E and M were conserved through shell crossings. In the next section, we drop this assumption and investigate whether our previous results remain true.

3. Global effect of shell crossing

Since the sign of $\Delta = E - E_{\text{lim}}$ determines the binding property of the system, it is useful to give the final values of E and E_{lim} for each shell, labeled i, in terms of the initial R_i and M_i, reaching areal radius r after crossing shells, with

$$M(r(R,t),t) = M_i + \int dM_{\text{in}} - \int dM_{\text{out}} = M_i + \Delta M_i,$$

where the index "in" refers to inward crossing, "out" to outward crossing, j to the shells crossing shell i.

Using definition 12 and integrating Eq. (29) over all crossing shells, we get

$$E_{\text{lim}}(r) = E_{\text{lim}}(R_i) - \left[\left(1 + \frac{\Delta M_i}{M_i}\right)^{2/3} - 1\right]\frac{3M_i}{r_{\text{lim}}(R_i)}, \quad (38)$$

$$E(r) = E(R_i) - 8\pi\left[\int dr_{j,\text{in}} - \int dr_{j,\text{out}}\right]\frac{\rho(r_j)r_j^2}{r_{\times i}(r_j)}, \quad (39)$$

where $r_{\times i}$ is a crossing radius. Because of their qualitatively simple shell-crossing histories, we can look at the changes for three peculiar shells, singled out on Fig. 8: the innermost limit shell, the outermost limit shell, and the maximum E shell initially lying in the interior of the outermost limit shell.

The innermost limit shell will only be crossed by more bound shells exterior to it, so $\Delta M_1 > 0$ and

$$E(r(R_{\star 1})) = E(R_{\star 1}) - 8\pi\int dr_{j,\text{in}}\frac{\rho(r_j)r_j^2}{r_{\times 1}(r_j)}. \quad (40)$$

Since

$$\frac{1}{3}\left(\frac{\Delta M_1}{M_1}\right)^2 + \left(\frac{2}{3}\frac{\Delta M_1}{M_1}\right)^3 > 0 \quad (41)$$

$$\Leftrightarrow \left[\left(1 + \frac{\Delta M_1}{M_1}\right)^{2/3} - 1\right] < \frac{2}{3}\frac{\Delta M_1}{M_1} \quad (42)$$

and

$$-\frac{1}{r_{\times 1}(r_j)} < -\frac{1}{\max[r_{\times 1}(r_j)]} < -\frac{1}{r_{\text{lim}}(R_{\star 1})}, \quad (43)$$

as the innermost limit shell becomes a bound shell, we get that

$$\Delta[E - E_{\text{lim}}]_1 < 2\Delta M_1\left[\frac{1}{r_{\text{lim}}(R_{\star 1})} - \frac{1}{\max[r_{\times 1}(r_j)]}\right] < 0. \quad (44)$$

Thus, the innermost limit shell will globally shift outwards, following the qualitative analysis of Fig. 4.

In turn, the outermost limit shell will be only crossed by all the unbound shells interior to it, so

$$E(r(R_{\star\text{out}})) = E(R_{\star\text{out}}) + 8\pi\int dr_{j,\text{out}}\frac{\rho(r_j)r_j^2}{r_{\times\text{out}}(r_j)} \equiv E(R_{\star\text{out}}) + 2\frac{\Delta M_{\text{out}}}{\langle r_{\times\text{out}}\rangle(R_{\star\text{out}})}, \quad (45)$$

where ΔM_{out} is the positive mass loss of the outermost limit shell and $\langle r_\times\rangle$ is a reduced crossing radius. Note that, by construction, $M_{\text{out}} > M(R_{\star\text{out}}, t \to \infty) = M_{\text{out}} - \Delta M_{\text{out}} > 0$.

Now, supposing the density distribution remains finite, we can decompose the crossing of the outermost limit shell by all escaping inner shells into a series of infinitesimal shell crossings. Thus, following Eq. (31) we get

$$d[E - E_{\text{lim}}] = -8\pi dr_{j,\text{out}}\rho(r_{j,\text{out}})r_{j,\text{out}}^2 \times\left(\frac{1}{r_{\text{lim}}(M_{\star\text{out}}(t_{\times j}))} - \frac{1}{r_{\times\text{out}}(r_{j,\text{out}})}\right). \quad (46)$$

As all shells cross outwards[20] and

[20]Note that $R_{\star\text{out}}$ starts as a marginally bound shell well inside its limit radius.

$$\frac{1}{\langle r_{\times\mathrm{out}}\rangle(R_{\star\mathrm{out}})} > \frac{1}{r_{\mathrm{lim}}(\langle r_{\times\mathrm{out}}\rangle)} \geq \frac{1}{r_{\mathrm{lim}}(R_{\star\mathrm{out}})}, \tag{47}$$

then, in this case, we have

$$\Delta[E - E_{\mathrm{lim}}]_{\mathrm{out}} = 2\Delta M_{\mathrm{out}}\left[\frac{1}{\langle r_{\times\mathrm{out}}\rangle(R_{\star\mathrm{out}})} - \frac{1}{r_{\mathrm{lim}}(R_{\star\mathrm{out}})}\right] > 0. \tag{48}$$

Thus, the outermost limit shell will shift relatively inwards, following the qualitative analysis of Fig. 6.

Finally, the maximum E shell initially inside $R_{\star\mathrm{out}}$, or with horizontal tangent (its initial radius is R_{max}), will be only crossed inwards by all the shells starting with radii above it and having an E below $E(R_{\mathrm{max}}, t \to \infty)$, at the moment of crossing. This shell will then follow

$$\Delta[E - E_{\mathrm{lim}}]_{\mathrm{max}} < 2\Delta M_{\mathrm{max}}\left[\frac{1}{r_{\mathrm{lim}}(R_{\mathrm{max}})} - \frac{1}{\max[r_{\times\,\mathrm{max}}(r_j)]}\right] < 0, \tag{49}$$

similarly as for the innermost limit shell.

We summarize the main result of this section as follows.

Result 5.—Consider a Λ-LTB spacetime where shell crossing exists. Then the metric and extrinsic curvature are discontinuous and the discontinuity in E is given by (29). Furthermore, at $R_{\star\mathrm{out}}$, $\Delta[E - E_{\mathrm{lim}}]_{\mathrm{out}} > 0$ and, at R_{max}, $\Delta[E - E_{\mathrm{lim}}]_{\mathrm{max}} < 0$. □

4. Qualitative analysis of limit trapped matter shells

In this section, we argue that the results contained in Summary 1 remain true for the case where M and E are not conserved through shell crossing.

We discussed the behavior of the outermost limit shell $R_{\star\mathrm{out}}$ and of the outward escaping highest energy inner shell R_{max} in Sec. III D 3. As those determine the two separating shells $R_{t\star\mathrm{out}\infty}$ and $R_{\mathrm{free}\infty}$ studied above, their modifications by shell crossing will indicate that the effective limit shells are just displaced but obey the same general properties. We illustrate this on the open background example (Fig. 8), for which we separated the study of each limit shell.

In Fig. 9, we represent the construction of using the qualitative evolution of $R_{\star\mathrm{out}}$ and its neighboring shells from Eq. (48).

In Fig. 10, using the qualitative evolution of E_{max} and its neighboring shells from Eq. (49), we represent the construction of the inner trapper matter shell for open initial conditions. The subsequent modifications proceed from those qualitative changes and do not modify the formulations of the results from their counterparts in the model where both E and M are conserved between shell crossings.

In the case where E and M are not conserved, the effect of shell crossing on $R_{\star\mathrm{out}}$ given by Eq. (48) implies only that $R_{t\star\mathrm{out}\infty} < R_{t\star\mathrm{out}}$ without qualitative changes and

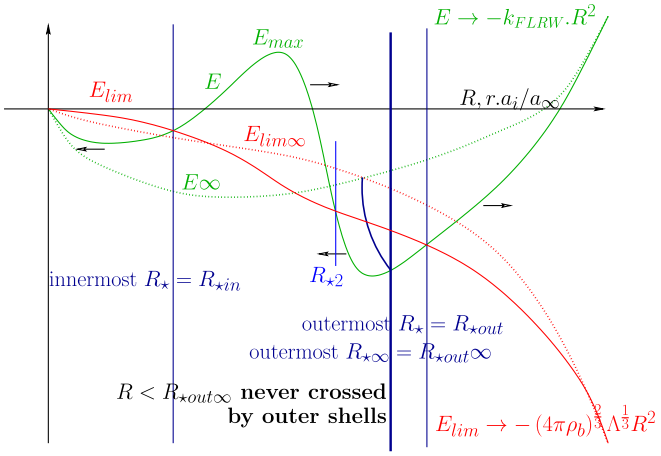

FIG. 9 (color online). Illustration, on an open background with arbitrary central mass distribution, of the effect of shell crossing on the inner global limit shell previously defined as the outermost local limit shell. The time variation of the locus of the outermost local limit shell leads to defining it as the time-infinity outermost limit shell: this is shown on the extrapolated time-infinity energy profiles and linked to the initial energy profile by a connecting curve. The global inner limit shell is then just shifted inwards, compared with the integrable analysis.

Definition 3 is verified. In turn, the effect of shell crossing on R_{free} depends on the effect on E_{free} from Eq. (49) and by the monotonous increase of E near infinity and only implies that $R_{\mathrm{free}\infty} < R_{\mathrm{free}}$.

Therefore, the findings of Sec. III D 2, extending the analysis of [5] in the context of shell crossing, are only quantitatively modified as full shell-crossing effects only

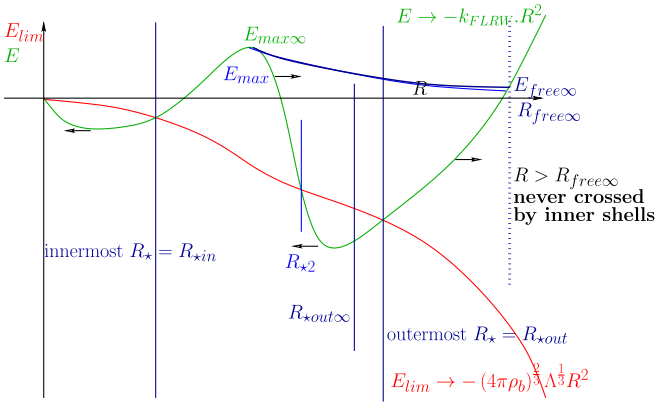

FIG. 10 (color online). Illustration, on an open background with arbitrary central mass distribution, of the effect of shell crossing on the outer global limit shell previously defined as the outer shell with same energy function as the inner shells' maximum. The time variations of the inner shells' maximum energy function from shell crossings lead to defining it as the outer shell with same energy as the time-infinity inner shells' maximum energy function E: this is shown with the highest of extrapolated time infinity Es of inner shells peaks. The global outer limit shell is then just shifted inwards, compared with the integrable analysis.

displace inwards both the inner and outer limit trapped matter shells: the initial outermost intersection of E and $E_{\rm lim}$ gets unbound and the system at infinity gets consequently reduced in Lagrangian initial radius. In turn, the maximum energy of the inner regions gets lowered, so the inner limit trapped matter surface is also drawn inwards. This displacement modifies only marginally the conclusions obtained in Sec. III D 2, namely: (i) the splitting of the local trapped matter shell is maintained when those shells exist. (ii) Open, flat, and closed models with *existing* $R_{t\star{\rm out}}$ [with $k_{\rm FLRW} < (4\pi\rho_b)^{2/3}\Lambda^{1/3}$] all retain an $R_{t\star{\rm out}\infty}$, and (iii) the modification of the maximum energy of the inner regions allows just more asymptotic cosmological flat models to keep their inner limit trapped matter shell, if the shift from $E_{\rm max}$ tends to $E_{\rm max\infty} < 0$.

Therefore, from the sufficient conditions for inner and outer limit trapped matter shells (Results 3 and 4), the results contained in Summary 1 remain true in the case where M and E are not conserved through shell crossing.

IV. EXAMPLES: NFW PROFILES WITH ONE UNDERCOMING INTERSECTION

In [5], we studied examples of trapped matter shells using cosmological models with a Navarro, Frenk, and White (NFW) density profile [30] and a simple parabolic E profile. Here we adapt those profiles in order to present one intersection with $E_{\rm lim}$ of the undercoming type as in the local configuration of Fig. 3, and thus ensure, at the local level, the appearance of shell crossing.

To do so, we use a fourth order polynomial in the canonical Lagrange form, to provide for the behavior in the intersecting region that we cut off with an exponential so that an open FLRW term dominates at infinity. We chose the profile to be 0 at the origin and at a characteristic radius R_0 set near the last possible intersection point with the NFW $E_{\rm lim}$ given by Eq. (4.21) of [5],

$$R_0 \leq R_{-1}, \qquad E_{\rm lim}(R_{-1}) = -1,$$

so as to secure the crossings in the physical region. The remaining three points of interpolation are chosen to be set alternately below and above the $E_{\rm lim}$ curve inside the region set by 0 and R_0. The form is set by

$$\begin{aligned} E(R) = \Big\{ & m_1 \frac{x}{x_1}\frac{x-x_2}{x_1-x_2}\frac{x-x_3}{x_1-x_3}\frac{x-1}{x_1-1} \\ & + m_2 \frac{x}{x_2}\frac{x-x_1}{x_2-x_1}\frac{x-x_3}{x_2-x_3}\frac{x-1}{x_2-1} \\ & + m_3 \frac{x}{x_3}\frac{x-x_1}{x_3-x_1}\frac{x-x_2}{x_3-x_2}\frac{x-1}{x_3-1} + \epsilon_1 x \Big\} e^{-x} \\ & - k_\infty R^2 \frac{\epsilon_0 x^2}{(x^2-1)\epsilon_0 + 1}, \end{aligned} \tag{50}$$

where $x = R/R_0$, we have denoted the three intermediate points as x_1, x_2, and x_3, the values of the polynomial at those points by m_1, m_2, and m_3, ϵ_1 is a small constant making sure we have the freedom to fit $E(R_0) = E(0) = 0$ where the polynomial itself is built to vanish, ϵ_0 is a small constant making sure the polynomial dominates in the interesting range but allowing the curvature at radial infinity to be set by a Friedmann-type k_∞. The form (50) automatically vanishes at 0. We chose the polynomial values such that at those points, E is alternately below, above, and again below $E_{\rm lim}$, the last one making sure it remains above -1:

$$E(R_0) = 0 = \epsilon_1 e^{-1} - k_\infty R_0^2 \epsilon_0, \quad \Rightarrow \epsilon_0 = \frac{\epsilon_1}{k_\infty R_0^2 e}, \tag{51}$$

$$\begin{aligned} E(R_1) = g E_{\rm lim}(R_1) &= (m_1 + \epsilon_1 x_1) e^{-x_1} - k_\infty R_0^2 \frac{\epsilon_0 x_1^4}{(x_1^2-1)\epsilon_0 + 1} = (m_1 + \epsilon_1 x_1) e^{-x_1} - \frac{\epsilon_1 x_1^4}{e - (1-x_1^2)\frac{\epsilon_1}{k_\infty R_0^2}} \\ \Rightarrow m_1 &= g E_{\rm lim}(R_1) e^{x_1} + \epsilon_1 x_1 \left(\frac{x_1^3 e^{x_1}}{e - (1-x_1^2)\frac{\epsilon_1}{k_\infty R_0^2}} - 1 \right), \end{aligned} \tag{52}$$

$$\begin{aligned} E(R_2) = \frac{E_{\rm lim}(R_2)}{g} &= (m_2 + \epsilon_1 x_2) e^{-x_2} - k_\infty R_0^2 \frac{\epsilon_0 x_2^4}{(x_2^2-1)\epsilon_0 + 1} = (m_2 + \epsilon_1 x_2) e^{-x_2} + \frac{\epsilon_1 x_2^4}{e - (1-x_2^2)\frac{\epsilon_1}{k_\infty R_0^2}} \\ \Rightarrow m_2 &= \frac{E_{\rm lim}(R_2)}{g} e^{x_2} + \epsilon_1 x_2 \left(\frac{x_2^3 e^{x_2}}{e - (1-x_2^2)\frac{\epsilon_1}{k_\infty R_0^2}} - 1 \right), \end{aligned} \tag{53}$$

$$\begin{aligned} E(R_3) &= E_{\rm lim}(R_3) - (E_{\rm lim}(R_3) + 1)(1-\epsilon) = (E_{\rm lim}(R_3) + 1)\epsilon - 1 = (m_3 + \epsilon_1 x_3) e^{-x_3} - k_\infty R_0^2 \frac{\epsilon_0 x_3^4}{(x_3^2-1)\epsilon_0 + 1} \\ &= (m_3 + \epsilon_1 x_3) e^{-x_3} + \frac{\epsilon_1 x_3^4}{e - (1-x_3^2)\frac{\epsilon_1}{k_\infty R_0^2}} \Rightarrow m_3 = [(E_{\rm lim}(R_3) + 1)\epsilon - 1] e^{x_3} + \epsilon_1 x_3 \left(\frac{x_3^3 e^{x_3}}{e - (1-x_3^2)\frac{\epsilon_1}{k_\infty R_0^2}} - 1 \right). \end{aligned} \tag{54}$$

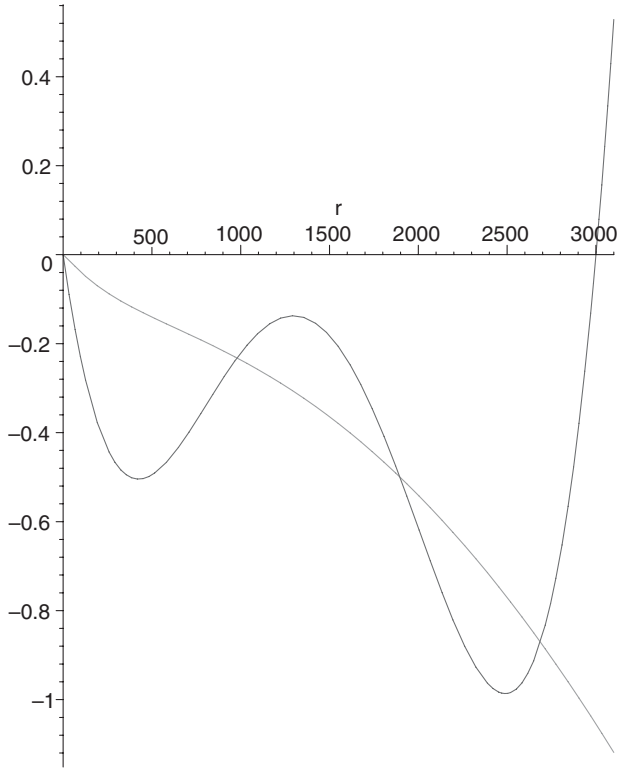

FIG. 11. NFW with background E_{lim} and an example of E profile given by Eqs. (50)–(54), setting $R_0 = 3000$, arbitrarily setting $x_1 = \frac{1}{4}$, $x_2 = \frac{1}{2}$, $x_3 = \frac{3}{4}$, $\epsilon_1 = 10^{-2}$, $g = 2$, and $\epsilon = e^{-1}$ so that the figure is proportioned.

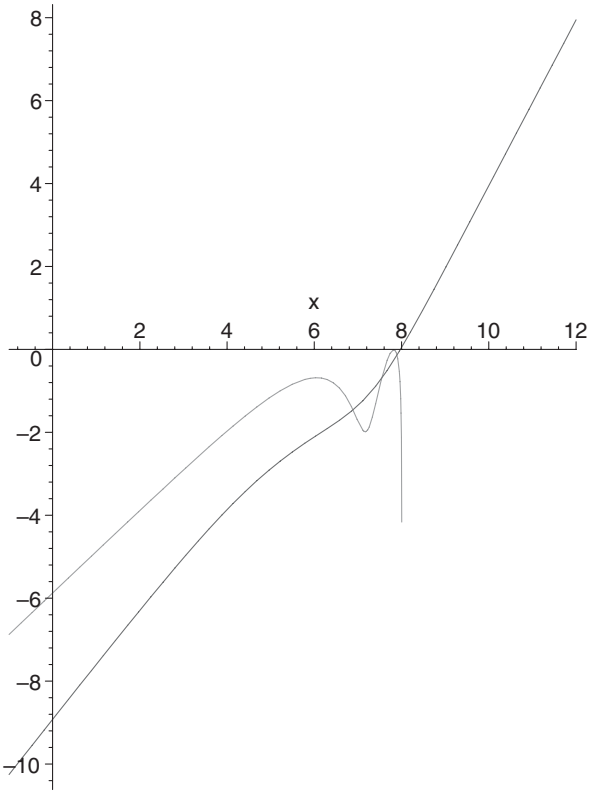

FIG. 12. NFW with background E_{lim} and an example of E profile given by Eqs. (50)–(54) in $\log(-E)$-$\log(-R)$ scale.

We illustrate this in Figs. 11 and 12 after choosing the values of the density profile identical to those in [5]. The cutoff leaves the region under R_0 almost unaffected by the Friedmann term, so the value of k_∞ is not very relevant there but we set it to -1.

We summarize the result of this section as:

Result 6.—For NFW density and initial data given by (50)–(54), the Λ-LTB spacetime has three shells $R_\star$ such that $E|_{R_\star} = E_{\mathrm{lim}}|_{R_\star}$. Furthermore, for this data, there is shell crossing and $R_{\star\mathrm{out}} - R_{\star\mathrm{out}\infty} < 0$ and $R_{\mathrm{free}} - R_{\mathrm{free}\infty} < 0$. □

V. CONCLUSIONS

We have studied the effects of shell crossing on the existence of trapped matter shells in Λ-LTB spacetimes. In particular, we have considered initial conditions such that: (i) our models approach a FLRW solution at radial infinity and have an initial outgoing Hubble-type flow; (ii) the shell crossing of dust remains pressureless and the mass of infinitely thin shells remains finite.

We have shown that the local trapped matter shells discussed in Ref. [5] split in two shells: one outer limit trapped matter shell and one inner limit trapped matter shell.

We have established sufficient conditions for the existence of such shells in Λ-LTB spacetimes, in terms of initial data for which shell crossing occurs. Furthermore, we have derived a number of properties for those shells using a qualitative approach inspired in Newtonian-like frameworks of cosmological kinematical models, as in [26,27].

We have also studied the role of shear in these settings and concluded, as in [17], that shear favors the emergence of trapped matter shells.

Finally, we have given concrete examples where shell crossing occurs and the inner and outer limit trapped matter shells emerge, using NFW data.

As potential applications of our models we note that (i) because of mass conservation and integrability in the absence of shell crossing at the boundary, the background asymptotic conditions remain FLRW over all time. Therefore, this gives an interesting setting to study the extendability of Birkhoff's theorem to cosmological expanding backgrounds; (ii) extensions of this work to unsmooth distributions of mass should be possible and might give support to current structure formation analyses using the spherical top hat collapse model, in the case of Λ-CDM.

ACKNOWLEDGMENTS

The work of M. LeD. is supported by CSIC (Spain) under Contract No. JAEDoc072, with partial support from CICYT Project No. FPA2006-05807, at the IFT,

Universidad Autonoma de Madrid, Spain. Financial support from the Portuguese Foundation for Science and Technology (FCT) under Contract No. PTDC/FIS/102742/2008 and Contract No. CERN/FP/109381/2009 is gratefully acknowledged by J. P. M. F. C. M. is supported by CMAT, Universidade do Minho, through FCT pluriannual funding, Projects No. PTDC/MAT/108921/2008 and No. CERN/FP/116377/2010 and Grant No. SFRH/BSAB/967/2010.

APPENDIX A: TIME-INFINITY DEFINITIONS

Definition 5.—The inner or nonbound shells of initial conditions in E and $E_{\rm lim}$, in the limit $t \to \infty$, induce a few remarkable features defined as follows:

(i) $R_{\star\infty} \equiv R_{\star i}(t \to \infty)$ is the intersection number i between $E(t \to \infty) = E_{\rm lim}(t \to \infty)$ taken at time infinity but singled out by its radius in the initial profile of E; in particular, we note $R_{\star{\rm out}\infty} \equiv R_{\star n}(t \to \infty)$ for the outermost intersection and $R_{t\star{\rm out}\infty} \equiv R_{\star{\rm out}\infty}$ when we add the condition $(E'(t \to \infty) > E'_{\rm lim}(t \to \infty))$.

(ii) We will note $E_{\max\infty}$ the maximum value taken at time infinity, but singled out in the initial profile, of nonbound E in the set of shells inside $R_{\star{\rm out}\infty}$ or outside but with initial horizontal tangent, i.e. $E_{\max\infty} = \{E, \max(E(t\to\infty)) \wedge ((E'=0) \vee (0 < R \le R_{\star{\rm out}\infty})) \wedge (E \ge E_{\rm lim})\}$.

(iii) $R_{\max\infty}$ is the largest value for which $E = E_{\max\infty}$, i.e. $R_{\max\infty} = \max\{R, E(R) = E_{\max\infty}\}$.

(iv) $R_{{\rm free}\infty}$, if it exists, is the furthest shell outside $R_{\star{\rm out}\infty}$ with an increasing E at $E = E_{\max\infty}$, i.e. $R_{{\rm free}\infty} = \max\{R, (R \ge R_{\star{\rm out}\infty}) \wedge (E = E_{\max\infty}) \wedge (E'(R) > 0)\}$.

(v) We will note $E_{{\rm free}\infty}$ the value of E, if it exists, such as $E_{{\rm free}\infty} = E(T = 0, R_{{\rm free}\infty})$. □

APPENDIX B: GAUGE INVARIANT DEFINITIONS FOR INNER LIMIT TRAPPED MATTER SHELLS

We can rewrite E in terms of gauge invariant quantities with Eqs. (9), (8), (14), (12), and (11):

$$\mathcal{L}_n\left(\frac{\Theta}{3} + a\right) \equiv \left(\frac{\dot r}{r}\right)^{\cdot} = \frac{1}{r^2}\left(\frac{r_{\rm lim}}{r} E_{\rm lim} - E\right)$$
$$\Leftrightarrow E(R) = \frac{r_{\rm lim}}{R} E_{\rm lim} - R^2 \mathcal{L}_n\left(\frac{\Theta}{3} + a\right)$$
$$= r^2\left(\frac{E_{\rm lim} r_{\rm lim}}{r^3} - \mathcal{L}_n\left(\frac{\Theta}{3} + a\right)\right),$$

so the condition of existence for $E_{\max}$, that $E \ge E_{\rm lim}$, translates into the initial condition with the inequality

$$\mathcal{L}_n\left(\frac{\Theta}{3} + a\right) = \frac{(\frac{r_{\rm lim}}{R} - 1)E_{\rm lim}}{R^2} + \frac{1}{R^2}(E_{\rm lim} - E)$$
$$\le \frac{(\frac{r_{\rm lim}}{R} - 1)E_{\rm lim}}{R^2} < 0,$$

or at time infinity into

$$\mathcal{L}_n\left(\frac{\Theta}{3} + a\right)\Big|_{(t\to\infty)} \le \frac{(\frac{r_{\rm lim}}{r} - 1)E_{\rm lim}}{r^2}\Big|_{(t\to\infty)} < 0.$$

We get then $R_{\max}$ and $E_{\max}$ from

$$R_{\max} = \max\left\{R, \frac{E}{R^2} = -\min\left\{\mathcal{L}_n\left(\frac{\Theta}{3} + a\right) - \frac{E_{\rm lim} r_{\rm lim}}{R^3}\right\} \wedge ((E'=0) \vee (0 < R \le R_{\star{\rm out}})) \wedge \left(\mathcal{L}_n\left(\frac{\Theta}{3} + a\right) \le \frac{(\frac{r_{\rm lim}}{R} - 1)E_{\rm lim}}{R^2} < 0\right)\right\}$$
$$\Rightarrow E_{\max} = -R_{\max}^2 \min\left\{\mathcal{L}_n\left(\frac{\Theta}{3} + a\right) - \frac{E_{\rm lim} r_{\rm lim}}{R^3}\right\} = \max\left\{R^2\left(\frac{E_{\rm lim} r_{\rm lim}}{R^3} - \mathcal{L}_n\left(\frac{\Theta}{3} + a\right)\right),\right.$$
$$\left.((E'=0) \vee (0 < R \le R_{\star{\rm out}})) \wedge \left(\mathcal{L}_n\left(\frac{\Theta}{3} + a\right) \le \frac{(\frac{r_{\rm lim}}{R} - 1)E_{\rm lim}}{R^2} < 0\right)\right\}.$$

Taken at $t \to \infty$, this translates into

$$R_{\max\infty} = \max\left\{R, E = \max\left\{-r^2\left(\mathcal{L}_n\left(\frac{\Theta}{3} + a\right) - \frac{E_{\rm lim} r_{\rm lim}}{R^3}\right)\Big|_{(t\to\infty)}\right\} \wedge ((E'=0) \vee (0 < R \le R_{\star{\rm out}\infty}))\right.$$
$$\left. \wedge \left(\mathcal{L}_n\left(\frac{\Theta}{3} + a\right) \le \frac{(\frac{r_{\rm lim}}{r} - 1)E_{\rm lim}}{r^2} < 0\right)\Big|_{(t\to\infty)}\right\}$$
$$\Rightarrow E_{\max\infty} = \max\left\{r^2\left(\frac{E_{\rm lim} r_{\rm lim}}{r^3} - \mathcal{L}_n\left(\frac{\Theta}{3} + a\right)\right)\Big|_{(t\to\infty)},\ ((E'=0) \vee (0 < R \le R_{\star{\rm out}\infty})) \wedge \left(\mathcal{L}_n\left(\frac{\Theta}{3} + a\right) \le \frac{(\frac{r_{\rm lim}}{r} - 1)E_{\rm lim}}{r^2} < 0\right)\Big|_{(t\to\infty)}\right\}.$$

Thus, Definition 4 can be rewritten as follows.

Definition 6.—Suppose that $E_{\max\infty}$ defined as

$$E_{\max\infty} = \max\left\{ r^2\left(\frac{E_{\lim} r_{\lim}}{r^3} - \mathcal{L}_n\left(\frac{\Theta}{3} + a\right)\right)\Big|_{(t\to\infty)}, \quad ((E' = 0) \vee (0 < R \leq R_{\star \mathrm{out}\infty})) \wedge \left(\mathcal{L}_n\left(\frac{\Theta}{3} + a\right) \leq \frac{(\frac{r_{\lim}}{r} - 1)E_{\lim}}{r^2} < 0\right)\Big|_{(t\to\infty)} \right\}, \tag{B1}$$

exists. Then, inner limit trapped matter shells are defined, in the models considered with GLTB coordinates, as the locus $R_{\mathrm{free}\infty}$ such that

$$R_{\mathrm{free}\infty} = \max\left\{ R, (R \geq R_{\star \mathrm{out}\infty}) \wedge \left(\frac{\Theta}{3} + a = \sqrt{\frac{E_{\max\infty}}{r^2} + 2\frac{M}{r^3} + \frac{1}{3}\Lambda}\right)_{t\to\infty} \wedge (E'(t \to \infty, R) > 0) \right\}. \tag{B2}$$

□

[1] F. Bernardeau, S. Colombi, E. Gaztanaga, and R. Scoccimarro, Phys. Rep. **367**, 1 (2002).
[2] D. F. Mota and C. van de Bruck, Astron. Astrophys. **421**, 71 (2004).
[3] M. Le Delliou, J. Cosmol. Astropart. Phys. 01 (2006) 021.
[4] I. Maor, Int. J. Theor. Phys. **46**, 2274 (2007).
[5] J. P. Mimoso, M. Le Delliou, and F. C. Mena, Phys. Rev. D **81**, 123514 (2010).
[6] C. Hellaby and K. Lake, Astrophys. J. **290**, 381 (1985).
[7] R. Sussman, Classical Quantum Gravity **27**, 175001 (2010).
[8] R. A. Sussman and G. Izquierdo, Classical Quantum Gravity **28**, 045006 (2011).
[9] S. M. C. Gonçalves, Phys. Rev. D **63**, 124017 (2001).
[10] K. Bolejko, A. Krasinski, and C. Hellaby, Mon. Not. R. Astron. Soc. **362**, 213 (2005).
[11] R. P. A. C. Newman, Classical Quantum Gravity **3**, 527 (1986).
[12] B. C. Nolan, Classical Quantum Gravity **20**, 575 (2003).
[13] D. Nunez, H. P. de Oliveira, and J. Salim, Classical Quantum Gravity **10**, 1117 (1993).
[14] S. M. C. Gonçalves, Phys. Rev. D **66**, 084021 (2002).
[15] P. D. Lasky and A. W. C. Lun, Phys. Rev. D **74**, 084013 (2006).
[16] C. W. Misner and D. H. Sharp, Phys. Rev. **136**, B571 (1964).
[17] A. Di Prisco, L. Herrera, E. Fuenmayor, and V. Varela, Phys. Lett. **A195**, 23 (1994); A. Abreu, H. Hernandez, and L. A. Nunez, Classical Quantum Gravity **24**, 4631 (2007); A. Di Prisco, L. Herrera, and V. Varela, Gen. Relativ. Gravit. **29**, 1239 (1997); L. Herrera and N. O. Santos, Phys. Rep. **286**, 53 (1997).
[18] S. S. Deshingkar, S. Jhingan, A. Chamorro, and P. S. Joshi, Phys. Rev. D **63**, 124005 (2001).
[19] S. M. C. Gonçalves, Phys. Rev. D **63**, 064017 (2001).
[20] F. C. Mena, B. Nolan, and R. Tavakol, Phys. Rev. D **70**, 084030 (2004).
[21] Y. B. Zeldovich and L. P. Grishchuk, Mon. Not. R. Astron. Soc. **207**, 23 (1984), http://adsabs.harvard.edu/abs/1984MNRAS.207P..23Z.
[22] K. Lake, Phys. Rev. D **29**, 1861 (1984).
[23] A. Meszaros, Mon. Not. R. Astron. Soc. **253**, 619 (1991), http://adsabs.harvard.edu/abs/1991MNRAS.253..619M.
[24] L. D. Landau and E. M. Lifshitz, *The Classical Theory of Fields* (Pergamon, New York, 1975), http://adsabs.harvard.edu/abs/1975ctf..book.....L.
[25] C. Hellaby and K. Lake, Astrophys. J. **282**, 1 (1984).
[26] S. F. Shandarin and Ya. B. Zel'Dovich, Rev. Mod. Phys. **61**, 185 (1989).
[27] P. Sikivie, I. I. Tkachev, and Y. Wang, Phys. Rev. D **56**, 1863 (1997).
[28] M. Le Delliou, Ph.D. thesis, Queen's University, Kingston, Canada, 2001, http://adsabs.harvard.edu/abs/2002PhDT.....7L.
[29] M. Le Delliou, Astron. Astrophys. **490**, L43 (2008).
[30] J. F. Navarro, C. S. Frenk, and S. D. M. White, Astrophys. J. **462**, 563 (1996).
[31] P. Sikivie, Phys. Rev. D **60**, 063501 (1999).